

Developing an efficient and visible prime editing system to restore tobacco 8-hydroxy-copalyl diphosphate gene for labdane diterpene Z-abienol biosynthesis

Jianduo Zhang^{1†}, Lu Zhang^{2†}, Chengwei Zhang^{2†}, Yongxing Yang², Huayin Liu³, Lu Li², Shengxue Zhang⁴, Xianggan Li⁴, Xinxiang Liu², Ya Liu², Jin Wang¹, Guangyu Yang¹, Qingyou Xia^{5*}, Weiguang Wang^{3*} & Jinxiao Yang^{2*}

¹Yunnan Key Laboratory of Tobacco, Yunnan Academy of Tobacco Science, Kunming 650231, China;

²Beijing Key Laboratory of Maize DNA Fingerprinting and Molecular Breeding, Beijing Academy of Agriculture & Forestry Sciences, Beijing 100089, China;

³Key Laboratory of Natural Products Synthetic Biology of Ethnic Medicinal Endophytes, State Ethnic Affairs Commission, Yunnan Minzu University, Kunming 650031, China;

⁴Cropedit Biotechnology Co. Ltd., Beijing 102206, China;

⁵Biological Science Research Center, Southwest University, Chongqing 400716, China

Received March 13, 2023; accepted May 30, 2023; published online July 14, 2023

Prime editing (PE) is a versatile CRISPR-Cas based precise genome-editing platform widely used to introduce a range of possible base conversions in various organisms. However, no PE systems have been shown to induce heritable mutations in tobacco, nor in any other dicot. In this study, we generated an efficient PE system in tobacco that not only introduced heritable mutations, but also enabled anthocyanin-based reporter selection of transgene-free T₁ plants. This system was used to confer Z-abienol biosynthesis in the allotetraploid tobacco cultivar HHDJY by restoring a G>T conversion in the *NtCPS2* gene. High levels of Z-abienol were detected in the leaves of homozygous T₁ plants at two weeks after topping. This study describes an advance in PE systems and expands genome-editing toolbox in tobacco, even in dicots, for use in basic research and molecular breeding. And restoring biosynthesis of Z-abienol in tobacco might provide an efficient way to obtain Z-abienol in plants.

prime editing, Z-abienol biosynthesis, visible marker, CRISPR, Cas9, tobacco

Citation: Zhang, J., Zhang, L., Zhang, C., Yang, Y., Liu, H., Li, L., Zhang, S., Li, X., Liu, X., Liu, Y., et al. (2023). Developing an efficient and visible prime editing system to restore tobacco 8-hydroxy-copalyl diphosphate gene for labdane diterpene Z-abienol biosynthesis. *Sci China Life Sci* 66, 2910–2921. <https://doi.org/10.1007/s11427-022-2396-x>

INTRODUCTION

Gene mutations are the molecular basis of elite trait variations. Mutations may cause gain or loss of gene function or changes in gene or protein expression. Clustered regularly interspaced short palindromic repeats (CRISPR)-CRISPR-

associated nuclease 9 (Cas9)-based genome editing systems have been developed quickly and applied widely to generate targeted mutations in various organisms and cell types (Anzalone et al., 2020; Gao, 2021). Such systems have the advantages of simple operation and high efficiency. Mutations induced by CRISPR/Cas9-based systems include not only gene knockouts, but also precise base substitution, which can be achieved with either of two effective systems: base editors (BEs) or prime editing (PE).

†Contributed equally to this work

*Corresponding authors (Qingyou Xia, email: xiaqy@swu.edu.cn; Weiguang Wang, email: wwg@live.cn; Jinxiao Yang, email: yangjinxiao@maizedna.org)

PE is more versatile than BEs, because it can be used to perform all twelve irreversible transition and transversion mutations. PE has therefore been developed rapidly in some monocotyledonous plants, such as rice, wheat, and maize, after its use was first reported in human cells (Hua et al., 2020; Jiang et al., 2020; Li et al., 2020; Lin et al., 2020; Tang et al., 2020; Xu et al., 2020a; Xu et al., 2020b). However, reports of PE systems are relatively limited in dicots, especially in stably transgenic plants. Most PEs have been tested in the context of transient transformation systems, in species including *Arabidopsis thaliana* (Jiang et al., 2022b; Yuan et al., 2021), *Nicotiana tabacum* (tobacco) (Wang et al., 2021), peanut, chickpea, and cowpea (Biswas et al., 2022). Transgenic plants using PE have only been regenerated in potato and tomato, but the editing efficiencies are very low and mutations are regarded as rarely heritable chimeras (Lu et al., 2021; Perroud et al., 2022).

In addition, unlike traditional transgenic plants that rely on transfer DNA (T-DNA), CRISPR-Cas based gene-edited plants with no exogenous T-DNA are welcomed, not only because T-DNA may produce additional unnecessary mutations and the location of the insertion site may cause undesirable side effects, but also because T-DNA must then be eliminated in a downstream commercial procedure. Screening transgene-free edited plants after the T₀ generation through genotyping or other detection methods is laborious and time-consuming (Yan et al., 2021). Reporter or selection systems, such as fluorescence markers (Dong et al., 2018; Gao et al., 2016; Wang et al., 2021; Yan et al., 2021), anthocyanin markers (Chen et al., 2022; Liu et al., 2019), and “suicide” transgenes that can cause plant self-elimination (He et al., 2018), have been used to solve this problem. Visible marker systems seem to be more popular, because it is most convenient to screen plants with the naked eye, especially in field conditions (Chen et al., 2022; Liu et al., 2019; Xu et al., 2021). Visible markers used with the CRISPR-Cas knockout system have greatly reduced the workloads required for selection of transgene-free plant after the T₀ generation (Gao et al., 2016; Liu et al., 2019; Yan et al., 2021). However, no PE system with a visible marker has yet been reported.

Z-abienol, a labdanoid diterpene found in balsam fir (*Abies balsamea*), Bolivian sunroot, and tobacco, functions in plant disease resistance (Seo et al., 2012). Z-abienol also imparts flavor and aroma characteristics to most oriental tobaccos (Leffingwell, 1999; Severson et al., 1984; Severson et al., 1985). More importantly, Z-abienol can be used as a starting material for semi-synthesis of amber compounds such as Ambrox[®], a widely-used and highly-priced compound that has replaced ambergris in the fragrance industry due to its delicate odor and fixative properties (Barrero et al., 1993; Zerbe and Bohlmann, 2015). Tobacco has greater potential than balsam fir or Bolivian sunroot for use as a Z-abienol-

producing bio-factory. Although most oriental tobaccos and cigars can synthesize Z-abienol, the majority of the commonly cultivated tobaccos throughout the world lack Z-abienol. Researchers have attempted to use transgenic approaches to allow non-producing cultivars to synthesize Z-abienol (Sallaud et al., 2012; Wang, 2016). They first uncovered *NtCPS2* and *NtABS*, which encode the two key enzymes involved in Z-abienol biosynthesis in tobacco (Sallaud et al., 2012). *NtCPS2* synthesizes 8- α -hydroxycopalyl diphosphate (8-OH-CPP) from geranylgeranyl diphosphate (GGPP) in glandular trichomes, and *NtABS* produces Z-abienol from 8-OH-CPP. Z-abienol was successfully synthesized in *Nicotiana sylvestris*, a wild diploid tobacco species, when *NtCPS2* and *NtABS* were co-expressed under the control of trichome-specific promoter of the CBT-ol synthase gene (Sallaud et al., 2012). Efforts were also made to biosynthesize Z-abienol in tobacco cv. Honghuadajinyuan (HHDJY), a commonly cultivated allotetraploid tobacco, through simultaneous overexpression of *NtCPS2* and *NtABS* under the control of the cauliflower mosaic virus (CaMV) 35S promoter, but this approach failed (Wang, 2016).

In the present study, we developed three PE systems in tobacco and finally found the visible PE system was more efficient in the production of heritable mutations and screening of transgene-free T₁ plants. We then used this PE system to edit the main gene regulating Z-abienol biosynthesis in HHDJY *in situ*, successfully enabling Z-abienol biosynthesis in this cultivar.

RESULTS

An efficient PE-Nt3-RT-M strategy in tobacco

Cas9 nickase (Cas9n) and the reverse transcriptase (RT) from Moloney murine leukemia virus (M-MLV) are two widely used and indispensable enzymes in PE systems. Since efficient PE systems are established by fusing RT to the C-terminus of Cas9n (Cas9n-M-MLV) in both human cells and many plants (Anzalone et al., 2019; Lin et al., 2020; Xu et al., 2020b), we first tested this fusion type in tobacco. Based on our previously reported rice PE-P2 system (Xu et al., 2020b), the *ZmUbi1* promoter was replaced by a double CaMV 35S promoter (2×35S) with the translational enhancer dMac3 (Kusano et al., 2018) to express the Cas9n-M-MLV fusion protein. At the same time, pegRNA and nesgRNA (enhanced sgRNA for nicking the non-edited strand) were connected by tRNA sequence and simultaneously driven by the same *U6* promoter of *Arabidopsis*. This PE system was thus designated PE-Nt2 (Prime Editor- *Nicotiana tabacum* version 2) (Figure 1A).

Three separate target sites, in the *ALS* (LOC107814192), *ALS-like* (LOC107787457), *NIP2-1* (LOC107775952) genes in tobacco were chosen to assess the efficiency and accuracy

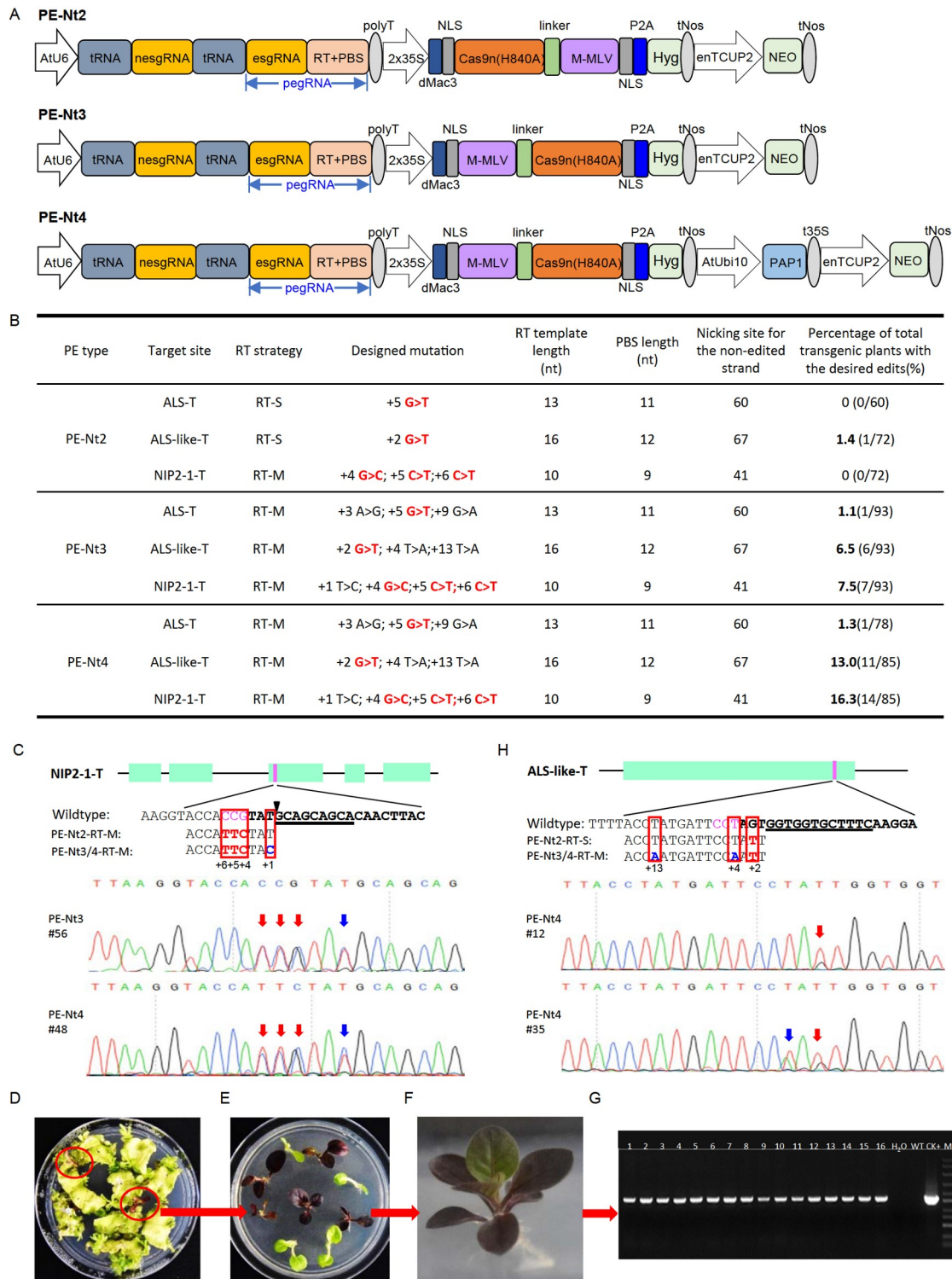


Figure 1 PE for precise genome editing in *T₀* tobacco plants. **A**, Schematic representation of the PE vectors PE-Nt2, PE-Nt3, and PE-Nt4. **B**, Summary of PE results for three PE systems in *T₀* plants. Each plant was sequenced using NGS. Desired base mutations are marked in red with the first 3' base of the pegRNA-induced nick as position +1. **C**, Schematic view of the NIP2-1-T target site and the sequence chromatogram showing multiple base mutations in the *T₀* plants of transgenic lines 56 and 48, which were generated by PE-Nt3 and PE-Nt4, respectively. The desired mutated bases are indicated with red arrows in the reverse strand. The assistant mutations are indicated with blue arrows. The pegRNA-induced nick is indicated with black inverted triangle. NGG PAM sequence is shown in pink. PBS sequence is underlined in black. **D**, Regenerated tobacco multiple shoots. Purple shoots are circled in red. **E**, *T₀* tobacco seedlings without roots. **F**, Representative purple *T₀* plant. **G**, Results of agarose gel electrophoresis demonstrating the transgenic status of representative purple *T₀* tobacco plants produced by one of three PE-Nt4 vectors. M, marker; WT, wild type *cv.* Samsun; CK+, PE-Nt4 vector. Samples from which a 1,552-bp fragment could be amplified were identified as transgenic. **H**, Schematic view of the ALS-like-T target site and the sequence chromatogram showing desired base mutations in *T₀* plants of transgenic lines 12 and 35, which were generated by PE-Nt4.

of the PE-Nt2 system (Figure 1B; Table S1 in Supporting Information). Each pegRNA contained a 9–12 nt primer binding site (PBS) and a 10–16 nt RT template (Figure 1B). The RT-template, which contained only a single desired nucleotide mutation, was termed as RT-S, while RT templates carrying multiple mutations were termed as RT-M. The three corresponding vectors were introduced into tobacco (*Nicotiana tabacum* L. cv. Samsun) by *Agrobacterium*-mediated transformation and 60, 72, and 72 transgenic T_0 plants were regenerated, respectively. Next-generation sequencing (NGS) of each T_0 plant identified undesired edits at the ALS-T target site and only one plant (line 22) successfully edited at the ALS-like-T target site, accounting for a low percentage of NGS reads (16.9%) (Figure 1B; Table S2 in Supporting Information). We then further confirmed this precise edit in line 22 using Sanger sequencing (Figure S1A in Supporting Information).

Our recent studies showed that higher PE efficiency could be obtained in rice and maize by fusing the M-MLV RT to the N terminus of Cas9n, especially in conjunction with the RT-M strategy that besides the desired single mutation, multiple synonymous base mutations nearby were introduced in RT template (Xu et al., 2022b). Based on these findings, we rearranged the Cas9n-M-MLV component of PE-Nt2 to generate the M-MLV-Cas9n fusion protein to generate the PE-Nt3 system (Prime Editor- *Nicotiana tabacum* version 3) (Figure 1A). Furthermore, RT-M strategy was also employed that not only the desired base mutations required to induce functional changes in phenotype, but also one or two additional synonymous base mutations (i.e., assistant mutations) were introduced to the RT template for each pegRNA of the PE-Nt3 system. This PE-Nt3-RT-M strategy was then tested in tobacco at the three targets described above. NGS analysis indicated that desired base mutations could be detected at all three targets with editing efficiencies of 1.1%, 6.5% and 7.5%, respectively (Figure 1B). Further analysis showed that among all 14 edited T_0 lines, 11 lines showed <20% NGS reads with desired mutation, while only one line (PE-Nt3: line 56) had >40% NGS reads with desired mutation at the NIP2-1-T target (Figure 1B; Table S2 in Supporting Information). Sanger sequencing was used to further confirm NGS results and showed that only independent T_0 lines with more than 12% desired edits NGS reads could be identified (Figure 1C; Figure S1 in Supporting Information). Taken together, these results indicated that the PE-Nt3-RT-M strategy was more efficient than PE-Nt2-RT-S strategy in tobacco.

More efficient visible PE-Nt4 system with RT-M strategy

Liu et al. (2019) employed the *PRODUCTION OF ANTHOCYANIN PIGMENTS 1* (*PAP1*) gene in Cas9 system to produce dark purple tobacco T_0 plants to improve the

knockout editing efficiency and facilitate selection of transgene-free T_1 plants. They also found that dark purple T_0 plants accumulated significantly higher levels of Cas9 transcript than those green T_0 plants without *PAP1* gene. We reasoned that the result of increasing Cas9 gene expression might also benefit for PE system in tobacco. In order to further improve the editing efficiency of PE system in tobacco we developed PE-Nt4 (Prime Editor- *Nicotiana tabacum* version 4) from the PE-Nt3 system (Figure 1A) by incorporating *PAP1* gene to produce an anthocyanin-assisted visual marker selection system, which might not only enrich more effective cells to improve prime editing efficiency, but also save cost and time when screening edited transgene-free T_1 plants.

Three PE-Nt4 related vectors were constructed using the same design as that in the PE-Nt3-RT-M strategy and used to transform *N. tabacum* cv. Samsun. As predicted, a certain number of purple tobacco shoots and plants were regenerated by all PE-Nt4 vectors (Figure 1D–F). We then selected 78, 85, and 85 purple T_0 plants for the ALS-T, ALS-Like-T, and NIP2-1-T targets respectively for PCR-based screening for each vector, among which, all plants were found to be transgene positive (Figure 1G). NGS of these transgenic purple plants indicated that the PE-Nt4 editing efficiency of desired edits was approximately twice that of PE-Nt3 at the ALS-like-T (13.0% vs. 6.5%) and NIP2-1-T (16.3% vs. 7.5%) targets, and showed similar efficiency at the ALS-T site (1.3% vs. 1.1%) (Figure 1B). Furthermore, four edits in T_0 plants (two at the ALS-like-T target site, lines 12 and 35, and two at NIP2-1-T, lines 17 and 48) accounted for >40% of desired mutation NGS reads (Table S3 in Supporting Information). Sanger sequencing was used to further confirm these NGS results and showed that only independent T_0 lines with at least 13% desired edits NGS reads could be identified (Figure 1C and H; Figure S1 in Supporting Information). These results suggested that the PE-Nt4-RT-M strategy was more efficient for prime editing in tobacco.

To investigate the off-target effect in the PE-Nt4 edited lines, we searched for the potential off-target sites sharing up to 5 mismatches with spacer sequences of pegRNAs for ALS-like-T and NIP2-1-T target sites. Finally, less than 3 mismatches could not be searched out. 8 and 5 potential off-target sites for ALS-like-T and NIP2-1-T spacer were chosen for further test respectively. And each top four T_0 plants with the highest desired-edits NGS reads percent at these two target sites were tested. No mutations were detected at all these selected off-target sites (Table S4 in Supporting Information).

PE-Nt4 editing of NtCPS2 confers Z-abienol biosynthesis in cv. HHDJY

In order to test whether the PE-Nt4-RM-T strategy could

create valuable traits in tobacco, we next considered suitable target genes for restoring function. Together, *NtCPS2* and *NtABS* are responsible for *Z*-abienol biosynthesis in tobacco (Figure 2A). However, this pathway might be disrupted in HHDJY (a main cultivated cultivar in Yunnan Province of China with high yield, quality and stress resistance), since it cannot produce *Z*-abienol. We therefore selected this cultivar for PE-based modification to try to restore *Z*-abienol production through PE-Nt4-RT-M *in situ* editing. Since previous studies found no polymorphisms in *NtABS* between *Z*-abienol producing and non-producing cultivars (Sallaud et al., 2012), we examined the HHDJY *NtCPS2* coding sequence for possible loss of function mutations. Sequence alignment between *Z*-abienol producing cultivar with HE588139.1 (Sallaud et al., 2012) and HHDJY revealed amino acid conversions at three different positions, one of which (caused by a G to T mutation in exon 4) generated a stop codon at position 98 in HHDJY (Figures S2 and S3 in Supporting Information). The G292T mutation in HHDJY was verified by Sanger sequencing of this region in both HHDJY and the *Z*-abienol producer, *cv.* Samsun (Figure 2B). This finding led us to hypothesize that restoring the T292G point mutation could confer *Z*-abienol biosynthesis in tobacco *cv.* HHDJY.

To first determine whether rescuing the G292T base mutation indeed resulted in *Z*-abienol biosynthesis, we expressed and purified N-terminal His-tagged HHDJY-*NtCPS2*-T292 and HHDJY-*NtCPS2*-T292G in *E. coli* (Wang

et al., 2020b) (Figure 2C). The two enzyme variants were then incubated with GGPP as substrate and the catalytic intermediates were analyzed by LC-MS to screen for labdene-diol, the de-phosphorylated product of 8-OH-CPP which serves as the precursor of *Z*-abienol (Sallaud et al., 2012). The results showed that only incubation with the HHDJY-*NtCPS2*-T292G protein resulted in labdene-diol accumulation *in vitro* (Figure 2D), thus confirming that the HHDJY-*NtCPS2*-T292G coding sequence could rescue the G292T conversion in *NtCPS2* gene restoring in HHDJY.

To then restore the *NtCPS2* function, we then employed the PE-Nt4-RT-M strategy to induce a T292G edit in the HHDJY genome. CPS2-T was designated as the target site and another two assistant mutations were designed in the RT template (Figure 3A; Table S1 in Supporting Information). Among 77 purple T₀ plants, two successfully edited plants (lines 10 and 17) were identified by Sanger sequencing (Figure 3A and B), and the *Z*-abienol contents in these lines were quantified by ACPI-LC-MS/MS. The results showed that *Z*-abienol could be detected in leaves of both lines at concentrations of 742.4 and 629.9 $\mu\text{g g}^{-1}$, respectively, while no *Z*-abienol was detected in a non-edited T₀ plant (T₀-WT) (Figure 3C; Table S5 in Supporting Information). These results demonstrated that restoring *NtCPS2* function *in situ* from the truncated form to full-length protein by PE-Nt4-mediated T to G conversion resulted in *Z*-abienol biosynthesis.

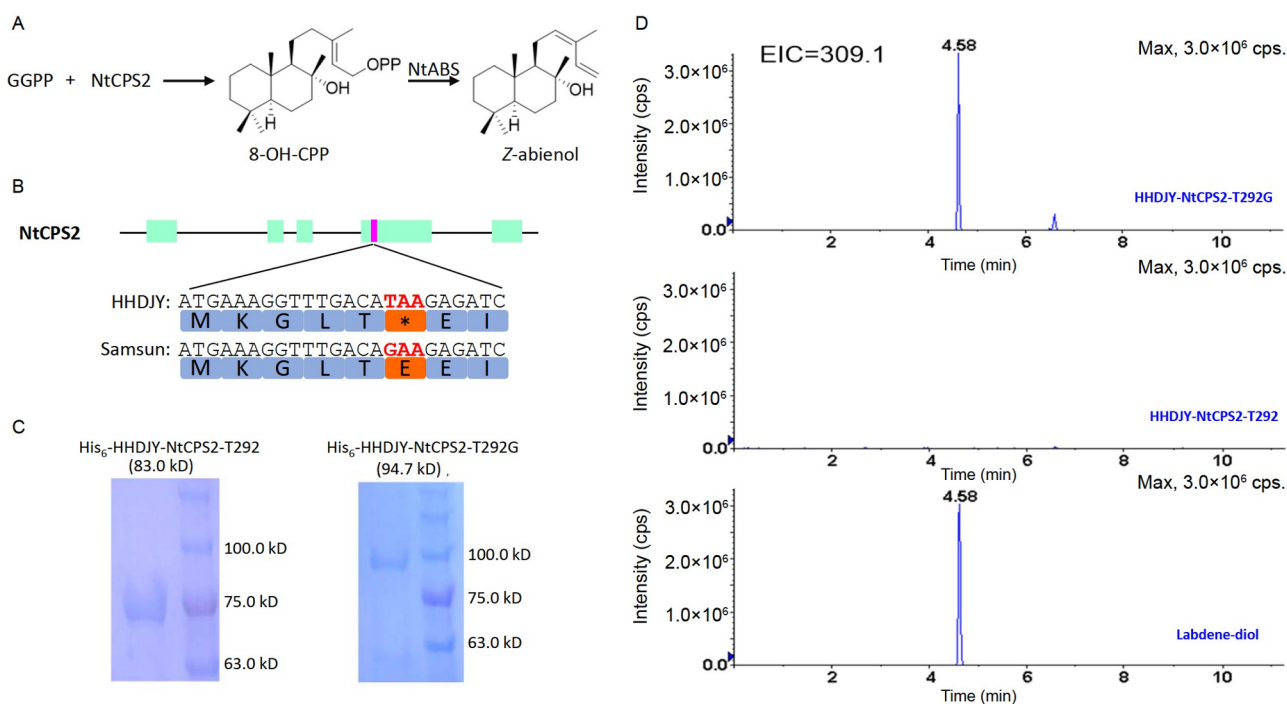


Figure 2 Functional verification of HHDJY-*NtCPS2*-T292G *in vitro*. **A**, Biosynthetic pathway of *Z*-abienol in tobacco. **B**, Sequence alignment of the *NtCPS2*-T292 site in wild-type HHDJY and Samsun. The codon containing the mutation is shown in red, and the corresponding amino acid residue is highlighted in orange. **C**, Sodium dodecyl-sulfate-polyacrylamide gel electrophoresis (SDS-PAGE) analysis of purified HHDJY-*NtCPS2*-T292 and HHDJY-*NtCPS2*-T292G. **D**, LC-APCI-MS/MS analysis of the enzymatic reaction products of HHDJY-*NtCPS2*-T292 and HHDJY-*NtCPS2*-T292G.

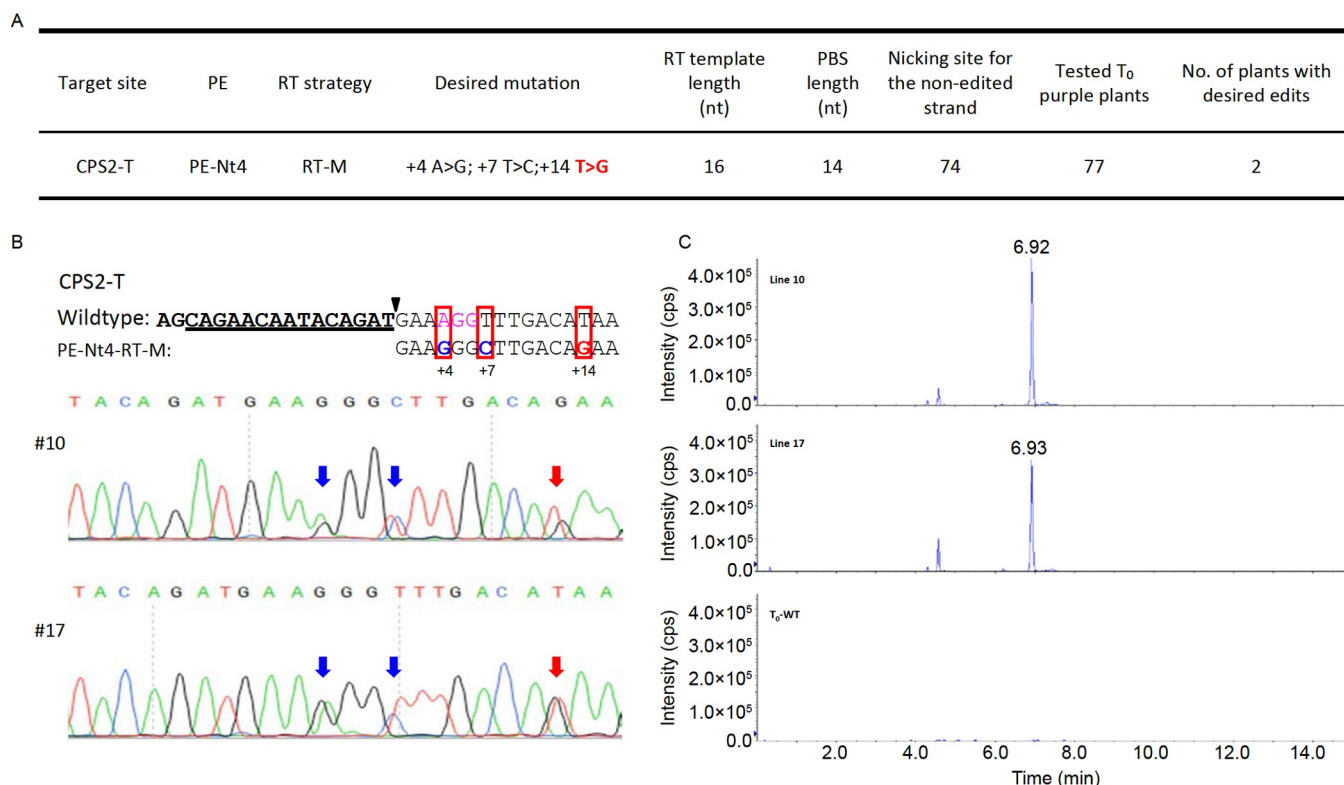


Figure 3 Enabling Z-abienol biosynthesis in HHDJY plants by restoring *NtCPS2* using the PE-Nt4-RT-M strategy. **A**, Summary of PE results using the PE-Nt4-RT-M strategy on CPS2-T target site in T₀ plants. Each plant was sequenced using Sanger sequencing. The desired base mutation is marked in red, with the first 3' base of the pegRNA-induced nick as position +1. **B**, Sequence chromatogram showing multiple base mutations at the CPS2-T target site in T₀ transgenic HHDJY lines 10 and 17, which were generated by the PE-Nt4-RT-M strategy. The desired mutated bases and assistant mutations are indicated with red and blue arrows, respectively. **C**, LC-APCI-MS/MS analysis of Z-abienol content in the leaves of T₀-WT, line 10, and line 17 plants.

Efficient screening for transgene-free *NtCPS2*-T292G-edited HHDJY T₁ lines

To screen for transgene-free T₁ plants, T₁ seeds of line 10 were planted in a hydroponic floating system. As expected, some T₁ plants were green and some were purple (Figure 4A). Leaf samples were obtained from 15 green and 15 purple plants at the four- or five-leaf stage (Figure 4A). PCR analysis to determine whether green plants were indeed transgene-free while purple plants were not shown that all detected purple plants carried the transgene, while almost all green plants (except plants #3 and #6) were transgene-free (Figure 4B). Consistent with these results, purple leaf midrib could be observed in plants #3 and #6 at the rosette stage after transplanting to larger pots (Figure S4 in Supporting Information). These collective results indicated that the PE-Nt4 reporter system based on anthocyanin production was highly effective for identifying transgene-free T₁ plants, especially in rosette stage. The *NtCPS2* T292G genotype was then screened in transgene-free green plants, which confirmed the presence of all three genotypes, including wild type, heterozygote and homozygote (Figure 4C) and showed that the T292G mutation in T₀ line 10 was faithfully inherited to the T₁ generation.

Z-abienol biosynthesis in HHDJY T₁ lines with functional *NtCPS2*-T292G

To determine whether the T292G mutation was inherited and could function in Z-abienol biosynthesis, Z-abienol was measured in the wild-type, heterozygous and homozygous T₁ green plants (T₁-WT, T₁-He and T₁-Ho) obtained from HHDJY plants edited in the above experiments. Leaf content of Z-abienol was detected at two weeks after topping, with Z-abienol producer Dabaijin-599 (Chang et al., 2018) serving as the positive control, and wild-type HHDJY used as the negative control for biosynthesis. APCI-LC-MS/MS analysis showed that Z-abienol accumulated in Dabaijin-599 (1,068.5 μg g⁻¹), while no Z-abienol was detected in wild-type HHDJY (Figure 4D, Table 1). In the T₁-Ho leaves, Z-abienol content reached 1,409.2, and 858.3 μg g⁻¹ in T₁-He leaves, while no Z-abienol was detectable in T₁-WT (Figure 4D, Table 1). At the same time, Z-abienol levels reached 1,372.0 μg g⁻¹ in the homozygous T₁ purple plants with T-DNA (T₁-Ho(T-DNA)), comparable with that in T₁-Ho leaves (Figure 4D, Table 1). These results indicated that T292G-edited *NtCPS2* was heritable and continued to function in Z-abienol biosynthesis in T₁ plants, and moreover, and the T-DNA label did not significantly

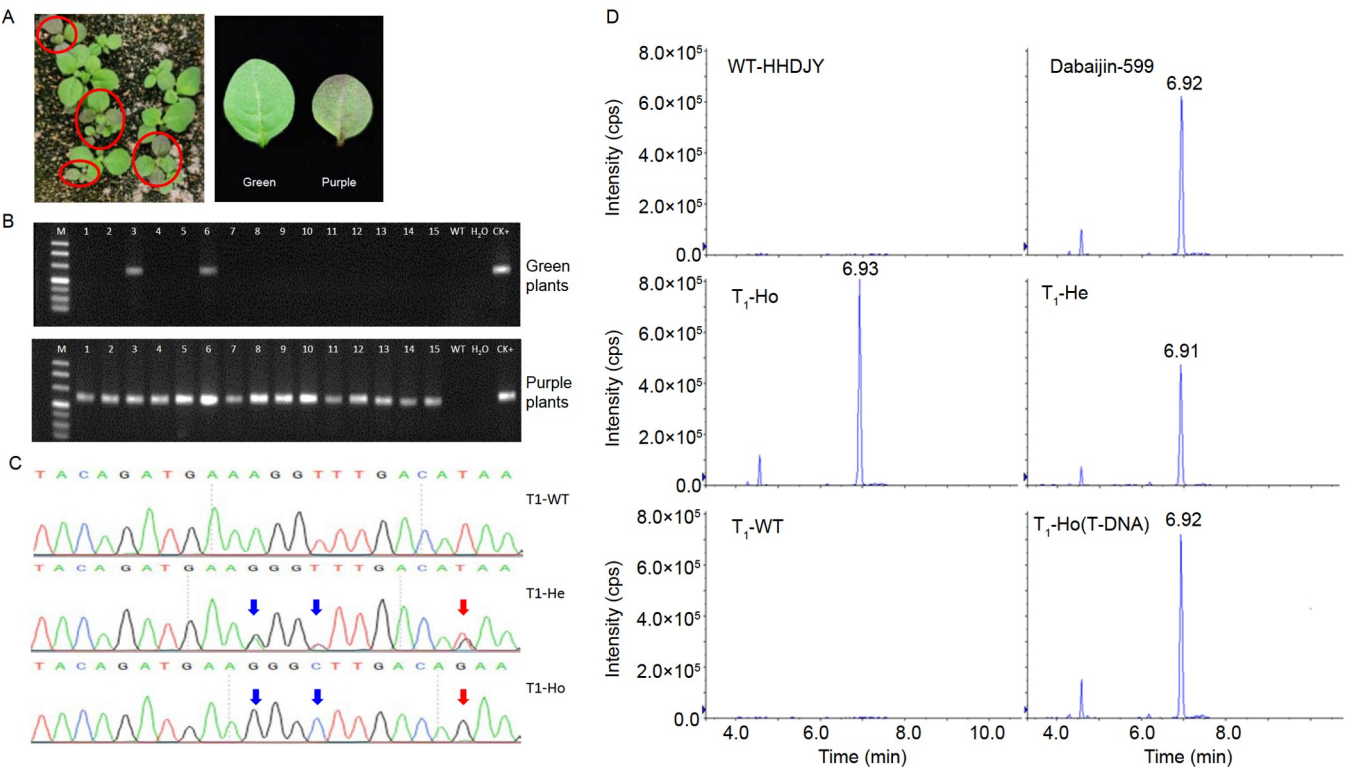


Figure 4 Efficient screening of transgene-free T₁ HHDJY plants and Z-abienol biosynthesis in NtCPS2-T292G-edited homozygotes and heterozygotes. A, T₁ plants derived from HHDJY T₀ line 10 in the tobacco floating system. Purple plants are circled in red. B, Agarose gel electrophoresis results from green and purple T₁ HHDJY plants. M, marker (bands from small to large are 50, 100, 150, 200, 300, 400, and 500 bp); WT, wild-type HHDJY; CK+, PE-Nt4 vector. Samples from which a 213-bp fragment could be amplified were identified as transgenic. C, Sequence chromatogram of three genotypes at the CPS2-T target site in transgene-free T₁ HHDJY plants. The desired mutated bases and assistant mutations are indicated with red and blue arrows, respectively. D, LC-APCI-MS/MS analysis of Z-abienol content in the leaves of wild type HHDJY (WT-HHDJY), Dabaijin-599, T₁-Ho, T₁-He, T₁-WT and T₁-Ho (T-DNA).

Table 1 Summary of Z-abienol content in multiple tobacco tissues at several growth stages

Plant	Tissue	Growth stage	Z-abienol (Repeat1) ($\mu\text{g g}^{-1}$)	Z-abienol (Repeat2) ($\mu\text{g g}^{-1}$)	Z-abienol (Repeat3) ($\mu\text{g g}^{-1}$)	Z-abienol Average ($\mu\text{g g}^{-1}$)
WT-HHDJY	Leaf	Topping	0	0	0	0
Dabaijin-599	Leaf	Topping	1,045.3	1,186.9	973.4	1,068.5
T ₁ -WT	Leaf	Topping	0	0	0	0
T ₁ -He	Leaf	Topping	816.5	913.2	845.2	858.3
T ₁ -Ho (T-DNA)	Leaf	Topping	1,401.8	1,372.4	1,341.7	1,372.0
T ₁ -Ho	Leaf	Topping	1,451.8	1,364.6	1,411.3	1,409.2
T ₁ -Ho	Leaf	Budding	642.9	705.3	717.8	688.7
T ₁ -Ho	Leaf	Rosette	400.6	376.2	365.5	380.8
T ₁ -Ho	Leaf	Seedling	91.4	128.5	114.6	111.5
T ₁ -Ho	Flower	Flowering	2,577.0	2,714.5	2,463.0	2,584.8
T ₁ -Ho	Sessile leaf	Topping	2,121.8	2,070.5	1,950.5	2,047.6
T ₁ -Ho	Stem epidermis	Topping	628.5	693.1	645.0	655.5
T ₁ -Ho	Leaf midrib	Topping	426.8	476.3	402.5	435.2

affect its expression.

Since Z-abienol accumulation may vary in different stages of tobacco growth, we next quantified Z-abienol production in leaves at different stages of T₁-Ho growth. In seedlings, Z-abienol content reached 111.5, 380.8 $\mu\text{g g}^{-1}$ at the rosette

stage, and 688.7 $\mu\text{g g}^{-1}$ at the budding stage (Table 1). Combined with our above results showing Z-abienol production of 1,409.2 $\mu\text{g g}^{-1}$ at two weeks after topping, these findings indicated that Z-abienol levels increased with plant growth age (Table 1). To test whether Z-abienol production

by T292G-edited *NtCPS2* occurred in different tissues, it was quantified in flowers, sessile leaves, leaf midrib, and stem epidermis of T₁-Ho, which revealed that production was highest in flowers (2,584.8 $\mu\text{g g}^{-1}$), followed by sessile leaves (2,047.6 $\mu\text{g g}^{-1}$), stem epidermis (655.5 $\mu\text{g g}^{-1}$), and lowest in the leaf midrib (435.2 $\mu\text{g g}^{-1}$) (Table 1). These results revealed that *Z*-abienol mainly accumulated in the leaves and flowers of tobacco plants, while its contents in the midrib and stem bark were relatively low. These results indicated that leaves are the most appropriate organs for obtaining *Z*-abienol since they have relatively high *Z*-abienol contents and comprise a substantially greater proportion of the total plant biomass than flowers. Taken together, all these findings illustrated that the PE-Nt4 system could be used for *in situ* editing to engineer natural product expression in tobacco.

DISCUSSION

The PE system is of great value for introducing precise base mutations into many organisms. We here successfully developed what is, to our knowledge, the first visible and mutation-heritable PE system (PE-Nt4) in dicots, specifically tobacco; most PE systems in dicots have been limited to transient transformations. The few dicots' PEs functioned in regenerated transgenic plants to date only induce chimeric mutations with extremely low editing efficiencies (Lu et al., 2021; Perroud et al., 2022). Therefore, our work not only expands the use of PE in tobacco for basic research and precise breeding applications, but also serves as a reference for future development of effective PEs in other dicots.

The strategy of combining PE-Nt3 with the introduction of assistant nucleotide substitutions in the RT template (PE-Nt3-RT-M) performed better than PE-Nt2. This was consistent with previous results in rice and maize (Xu et al., 2022b). There was no need to worry about assistant base mutations, because they were always designed to induce synonymous amino acid mutations to avoid any undesirable trait influences. The PE-Nt4-RT-M strategy outperformed PE-Nt3-RT-M strategy; PE-Nt4-RT-M not only showed higher target sequence editing efficiency, but also provided a convenient visible selection. All purple T₀ plants were transgenic and could be further detected their target mutation. The accuracy in identifying transgene-free T₁ plants was high, especially at the rosette stage (Figure 4B; Figure S4 in Supporting Information). This was consistent with a previous report in which the PAP1-related visual selection marker system was used for the accurate screening of tobacco non-transgenic T₁ plants produced by Cas9-PF (Liu et al., 2019). These data indicated that PAP1 may be a viable time- and labor-saving marker that could be widely used in CRISPR-Cas-related genome editing tools in tobacco to

screen T₁ plants. Our results also provide a reference for development of visible PE systems in other plant species. In addition, the PE-Nt4-RT-M strategy seemed producing fewer T₀ plants with undesired edits than the PE-Nt3-RT-M strategy (Tables S2 and S3 in Supporting Information). Based on these results, we suggest the PE-Nt4-RT-M strategy as the first choice for future use.

In addition, we found that a small portion of edits only have partial base mutations we designed in RT templates. For example, three base mutations (desired +2 G>T; assistant +4 T>A; assistant +13 T>A) were designed in RT templates at ALS-like-T target, but only one or two base mutations were induced in line 12 (desired +2 G>T) and line 35 (desired +2 G>T and assistant +4 T>A) by PE-Nt4 (Figure 1H). The same phenomenon was also found in our previous study (Xu et al., 2022b). Although the template was reverse transcribed by the M-MLV, how the reversed template was replaced to the genome remained unclear. We speculated that bases proximal to the nicking site would be easier to be edited than the distal. Thus, we suggest that it is better to design the desired nucleotide mutation proximal to the nicking site.

The PE-Nt4-RT-M strategy did not have high efficiency for inducing the desired base mutations, which were limited to NGG protospacer adjacent motif (PAM) sequences. Future work should focus on two areas. One area is improvement of editing efficiency, which could be tested with several strategies (Chen et al., 2021; Jiang et al., 2020; Jiang et al., 2022a; Li et al., 2022a; Li et al., 2022b; Lin et al., 2021; Nelson et al., 2022; Qiu et al., 2022; Zong et al., 2022; Zou et al., 2022), such as using PEmax, incorporating pegRNA with structured RNA motifs, using different promoters, using surrogate systems, inhibiting DNA mismatch repair (MMR), optimizing the length of PBS and RT templates, optimizing the Tm of PBS, or modifying the number and the position of assistant bases. The other area is expansion of the target scope by employing SpCas9 variants or Cas9 orthologs (Miller et al., 2020; Ren et al., 2021; Sretenovic et al., 2021; Tan et al., 2022; Walton et al., 2020; Wang et al., 2020a; Xu et al., 2022a; Zhang et al., 2020; Zhang et al., 2021). As for off-target effect, PE-Nt4-RT-M strategy did not induce any mutations at those selected potential off-target sites in tobacco. Jin et al. (2021) sequenced 29 PE-treated rice plants at the genome-wide level and confirmed that PEs do not induce genome-wide pegRNA-independent off-target single-nucleotide variants or small insertions/deletions. Given the low number of T₀ plants with relatively high desired on-target mutation NGS reads, PE-Nt4-RT-M strategy might act as the reported rice PEs and not induce genome-wide off-target effects in tobacco. However, it is better to analyze the off-target effect of PE-Nt4-RT-M strategy at the genome-wide level in the future, after all, tobacco is different from rice.

Using the PE-Nt4-RT-M strategy, we successfully syn-

thesized Z-abienol in HHDJY through an *in situ* T to G mutation at position 292 in exon 4 of *NtCPS2*. This is the first report of Z-abienol biosynthesis in allotetraploid tobacco via genetic engineering. Furthermore, this is the first report of inducing Z-abienol biosynthesis in plants using genome editing tools. Biosynthesis of Z-abienol in a key tobacco cultivar will allow sustainable production of large amounts of the precursor for the synthesis of Ambrox, which is highly valued in the fragrance industry. A previous report showed that Z-abienol failed to be synthesized in HHDJY when *NtCPS2* and *NtABS* genes were co-expressed under the CaMV 35S promoter (Wang, 2016). One of the failure reasons might be the expression level of CaMV 35S promoter in glandular trichomes was extremely lower than that of internal *NtCPS2* or *NtABS* promoter, while glandular trichomes were just the place where Z-abienol was synthesized *in vivo*. Another reason might be transgene silencing. *In situ* editing by PE-Nt4-RT-M strategy was a superior way to synthesize Z-abienol, since it would keep high expression level of the endogenous promoter in glandular trichomes to avoid transgene silencing and the difficulty of selecting trichome-specific promoter with high expression level.

Previous studies showed that *NtCPS2* was a key gene controlling Z-abienol biosynthesis in tobacco, and that the base at position 292 in exon 4 was an important single nucleotide polymorphism (SNP) (He et al., 2021; Sallaud et al., 2012). Our results showing that *in situ* T292G mutation in *NtCPS2* using the PE-Nt4-RT-M strategy conferred the ability to synthesize Z-abienol further confirmed these conclusions. Additionally, *in vitro* enzymatic reactions with *NtCPS2*-T292G demonstrated the function of this enzyme in synthesizing Z-abienol, consistent with previous results showing *NtCPS2* functionality (Sallaud et al., 2012). Notably, the present study confirmed that truncated *NtCPS2*-T292 was nonfunctional via *in vitro* enzymatic reactions for the first time.

Levels of Z-abienol in T₁-Ho (1,409.2 $\mu\text{g g}^{-1}$) were ~1.6-fold higher than they were in T₁-He (858.3 $\mu\text{g g}^{-1}$), showing an additive effect of *NtCPS2*. We also found that for T₁-Ho, Z-abienol content increased in the leaves as growth stages progressed through the seedling, rosette, budding, and topping stages. These findings were consistent with previous reports of diterpenoid accumulation in tobacco (Fu et al., 2019). Z-abienol is secreted by glandular hairs in tobacco, which are produced by many aerial tissues. Flowers showed the highest Z-abienol content, followed by sessile leaves, leaves, stem epidermis, and leaf midrib. These results were consistent with the distribution of glandular hair secretions in tobacco tissues (Fu et al., 2019). Based on these results, for optimal Z-abienol extraction, we suggest using the leaves of homozygous plants at two weeks after the topping stage.

The visible PE-Nt4 system described in this study paves the way for future use of PE in functional genomics research

and precision molecular breeding in tobacco. Furthermore, it may facilitate the development of similar tools in other plant species, especially dicots. Biosynthesis of Z-abienol in a main tobacco cultivar will be of great use, allowing continuous and abundant Z-abienol production. This result also sets a good example that besides traditional transgenic methods, *in situ* genome editing of key genes is a viable approach for synthesis of target products of plant secondary metabolism.

MATERIALS AND METHODS

Design of RT template and PBS

Target site sequences and the corresponding nearby sequences in Samsun were firstly identified using Sanger sequencing before designing each RT template and PBS. Primers were designed according to online tobacco genome database (https://www.ncbi.nlm.nih.gov/assembly/GCF_000715135.1/) and listed in Table S6 in Supporting Information. The identified target site sequences were shown in Table S1 in Supporting Information. The length of RT template and PBS, and the T_m of PBS in each pegRNA were designed based on principles described in the previous studies (Anzalone et al., 2019; Lin et al., 2021). In this study, the length of PBS was 9–12 nt and the length of RT template was 10–16 nt. PBS T_m was 30–40°C. The first base in the 3' extension of the RT template was not C. For assistant base design in the RT template, the principles were reported in our previous study (Xu et al., 2022b). One or two assistant bases inducing synonymous amino acids were introduced, and rare codons should be avoided. The positions of assistant bases can be anywhere besides the desired mutation base, but a closer position is preferred.

Plasmid construction

The previously-reported PE-P2-basic vector (Xu et al., 2020b) and PE-P3-basic vector (Xu et al., 2022b) were first digested with SnaBI and MfeI to obtain two independent fragments without ZmUbi1. They were then separately fused with a synthesized AtU6+tRNA+2×35S+dMac3 fragment using the NEBuilder HiFi DNA Assembly Master Mix (New England Biolabs, USA), yielding the PE-Nt2-basic-M vector and the PE-Nt3-basic-M vector. In both the PE-Nt2-basic-M and the PE-Nt3-basic-M vector, OsU6a was replaced with a synthesized enTCUP2+NEO+tNos fragment to generate the PE-Nt2-basic and PE-Nt3-basic vectors. In the PE-Nt3-basic-M vector, OsU6a was also replaced with a synthesized AtUbi10+PAP1+t35S+enTCUP2+NEO+tNos fragment to generate the PE-Nt4-basic vector. Three PE-Nt2 vectors were constructed as previously described for each PE-P2 vector (Xu et al., 2020b), and three PE-Nt3 vectors and four

PE-Nt4 vectors were constructed as previously described for each PE-P3 vector (Xu et al., 2022b). All primers for vector construction are listed in Table S7 in Supporting Information.

Tobacco transformation

The wild-type *Agrobacterium tumefaciens* strain GV3101 (Weidi Biotech, Shanghai, China) was transformed with each PE-Nt2, PE-Nt3, and PE-Nt4 construct using the freeze/thaw method, except for one CPS2-T target site-related PE-Nt4 construct, which was transformed into *Agrobacterium tumefaciens* EHA105 (Weidi Biotech). *Agrobacterium*-mediated transformation was then conducted on leaf discs from 2- to 3-week-old sub-cultured *N. tabacum* L. cv. Samsun and HHDJY plants as previously described (Horsch et al., 1985); Samsun leaf discs were incubated with each transformed GV3101 line, and HHDJY leaf discs were incubated with transformed EHA105. After incubation with *Agrobacterium* for 10 min, leaf discs recovered for 3 days, then were transferred to regeneration medium containing 50 mg L⁻¹ hygromycin (for Samsun) or 50 mg L⁻¹ kanamycin (for HHDJY) for 2 weeks. Leaf discs were sub-cultured on the same medium for 2–3 weeks to obtain multiple green or purple shoots. At 2–3 cm in length, shoots were transferred to rooting Murashige and Skoog (MS) medium with hygromycin or kanamycin (50 mg L⁻¹) for ~2 weeks to obtain T₀ plants with roots.

Identification of transgenic and transgene-free plants

Genomic DNA (gDNA) was extracted from each sampled T₀ or T₁ plant using the DNA Quick Plant System (Tiangen Biotech, Beijing, China). Target sequences were amplified using specific primers; samples were verified as transgenic T₀ or T₁ plants based on examination of the specific PCR products via agarose gel electrophoresis. Samples with no PCR product were identified as transgene-free T₁ plants. All primers used for this study and the related PCR product sizes are listed in Table S6 in Supporting Information.

Mutation identification

All identified transgenic T₀ plants, except for those related to Z-abienol biosynthesis, were first detected using NGS. Target regions were amplified from gDNA with site-specific primers (short) in the first round of PCR (Table S6 in Supporting Information). In the next round, forward barcodes were added to the ends of the PCR products using barcode primers (long) (Table S6 in Supporting Information). The PCR products were then sequenced at Tsingke Biotechnology Co., Ltd (Beijing, China) using the MiSeq platform to identify the mutations. Analysis of the PE mutation fre-

quency in each tested plant was performed using CRISPResso2 (<https://doi.org/10.1038/s41587-019-0032-3>). During data analysis, mutation reads lower than 5% were filtered. All T₀ plants with desired mutations identified by NGS analysis were further detected by Sanger sequencing. Target sequences were amplified with specific primers (Table S6 in Supporting Information) and Tsingke Biotechnology Co., Ltd performed Sanger sequencing on the PCR products. The Sanger sequencing chromatograms for each target site were analyzed using Vector NTI or SnapGene software. Mutant genotypes in both T₀ and T₁ plants produced by PE-Nt4 targeting CPS2-T were only detected via Sanger sequencing.

Off-target mutation detection

We used the local Cas-OFFinder (<https://doi.org/10.1093/bioinformatics/btu048>) to search for potential off-target sites. All NGG PAMs were searched in tobacco genome (PRJNA208209), and some off-target sites with no more than 5 mismatch bases were selected (Table S4 in Supporting Information). Four edited T₀ plants at ALS-like-T target site (Lines 12, 35, 19, 48) and four edited T₀ plants at NIP2-1-T target site (Lines 17, 74, 48, 85) were tested. Leaves from two T₀ plants were mixed together to be one sample. Finally, there were four samples, including line 12 and line 35, line 19 and line 48, line 17 and line 74, line 48 and line 85. PCR and NGS analysis were the same with those for mutation identification described above. Primers used for this study are listed in Table S4 in Supporting Information.

Expression and purification of HHDJY-NtCPS2-T292 and HHDJY-NtCPS2-T292G

The detailed method was listed in Method S1 in Supporting Information.

Enzymatic reaction assays of HHDJY-NtCPS2-T292 and HHDJY-NtCPS2-T292G

The detailed method was listed in Method S2 in Supporting Information.

Liquid chromatography-atmospheric pressure chemical ionization-tandem mass spectrometry (LC-APCI-MS/MS) analysis of Z-abienol in tobacco

The detailed method was listed in Method S3 in Supporting Information.

Compliance and ethics The authors submitted patent applications based on the results reported in this paper, and they declare that they have no conflict of interest.

Acknowledgements This work was supported by Beijing Scholars Program (BSP041), Financial Special Fund of Beijing Academy of Agriculture and Forestry Sciences (CZZJ202206), the key projects of YNZY (2022JY02) and CNTC (110202101034, JY-11). The authors thank Dr. Jiuran Zhao for helpful discussions and comments on the manuscript.

References

- Anzalone, A.V., Koblan, L.W., and Liu, D.R. (2020). Genome editing with CRISPR-Cas nucleases, base editors, transposases and prime editors. *Nat Biotechnol* 38, 824–844.
- Anzalone, A.V., Randolph, P.B., Davis, J.R., Sousa, A.A., Koblan, L.W., Levy, J.M., Chen, P.J., Wilson, C., Newby, G.A., Raguram, A., et al. (2019). Search-and-replace genome editing without double-strand breaks or donor DNA. *Nature* 576, 149–157.
- Barrero, A.F., Alvarez-Manzaneda, E.J., Altarejos, J., Salido, S., and Ramos, J.M. (1993). Synthesis of Ambrox® from (–)-sclareol and (+)-cis-abienol. *Tetrahedron* 49, 10405–10412.
- Biswas, S., Bridgeland, A., Irum, S., Thomson, M.J., and Septiningsih, E. M. (2022). Optimization of prime editing in rice, peanut, chickpea, and cowpea protoplasts by restoration of GFP activity. *Int J Mol Sci* 23, 9809.
- Chang, A.X., Qu, Y.F., Wang, G.P., Li, Y.Y., Luo, C.G., Feng, Q.F., Chen, Z.Q., Fu, X.K., Yang, A.G., Hu, R.S., et al. (2018). Study on key components and molecular basis responsible for the specific aroma traits of flue-cured tobacco Dabaijin599 (in Chinese). *Chin Tob Sci* 39, 1–9.
- Chen, C., Liu, X., Li, S., Liu, C., Zhang, Y., Luo, L., Miao, L., Yang, W., Xiao, Z., Zhong, Y., et al. (2022). Co-expression of transcription factors ZmC1 and ZmR2 establishes an efficient and accurate haploid embryo identification system in maize. *Plant J* 111, 1296–1307.
- Chen, P.J., Hussmann, J.A., Yan, J., Knipping, F., Ravisankar, P., Chen, P. F., Chen, C., Nelson, J.W., Newby, G.A., Sahin, M., et al. (2021). Enhanced prime editing systems by manipulating cellular determinants of editing outcomes. *Cell* 184, 5635–5652.e29.
- Dong, L., Li, L., Liu, C., Liu, C., Geng, S., Li, X., Huang, C., Mao, L., Chen, S., and Xie, C. (2018). Genome editing and double-fluorescence proteins enable robust maternal haploid induction and identification in maize. *Mol Plant* 11, 1214–1217.
- Fu, Q.J., Liu, Y.H., Du, Y.M., Wang, A.H., and Liu, X.M. (2019). Analysis of cembratriendiol content in tobaccos growing in China (in Chinese). *Acta Tab Sin* 25, 10–14.
- Gao, C. (2021). Genome engineering for crop improvement and future agriculture. *Cell* 184, 1621–1635.
- Gao, X., Chen, J., Dai, X., Zhang, D., and Zhao, Y. (2016). An effective strategy for reliably isolating heritable and Cas9-free *Arabidopsis* mutants generated by CRISPR/Cas9-mediated genome editing. *Plant Physiol* 171, 1794–1800.
- He, L., Liu, H., Cheng, C., Xu, M., He, L., Li, L., Yao, J., Zhang, W., Zhai, Z., Luo, Q., et al. (2021). RNA sequencing reveals transcriptomic changes in tobacco (*Nicotiana tabacum*) following NtCPS2 knockdown. *BMC Genomics* 22, 467.
- He, Y., Zhu, M., Wang, L., Wu, J., Wang, Q., Wang, R., and Zhao, Y. (2018). Programmed self-elimination of the CRISPR/Cas9 construct greatly accelerates the isolation of edited and transgene-free rice plants. *Mol Plant* 11, 1210–1213.
- Horsch, R.B., Fry, J.E., Hoffmann, N.L., Wallroth, M., Eichholtz, D., Rogers, S.G., and Fraley, R.T. (1985). A simple and general method for transferring genes into plants. *Science* 227, 1229–1231.
- Hua, K., Jiang, Y., Tao, X., and Zhu, J. (2020). Precision genome engineering in rice using prime editing system. *Plant Biotechnol J* 18, 2167–2169.
- Jiang, Y., Chai, Y., Qiao, D., Wang, J., Xin, C., Sun, W., Cao, Z., Zhang, Y., Zhou, Y., Wang, X.C., et al. (2022a). Optimized prime editing efficiently generates glyphosate-resistant rice plants carrying homozygous TAP-IVS mutation in *EPSPS*. *Mol Plant* 15, 1–4.
- Jiang, Y.Y., Chai, Y.P., Lu, M.H., Han, X.L., Lin, Q., Zhang, Y., Zhang, Q., Zhou, Y., Wang, X.C., Gao, C., et al. (2020). Prime editing efficiently generates W542L and S621I double mutations in two ALS genes in maize. *Genome Biol* 21, 257.
- Jiang, Z., Abdullah, Z., Zhang, S., Jiang, Y., Liu, R., and Xiao, Y. (2022b). Development and optimization of CRISPR prime editing system in photoautotrophic cells. *Molecules* 27, 1758.
- Jin, S., Lin, Q., Luo, Y., Zhu, Z., Liu, G., Li, Y., Chen, K., Qiu, J.L., and Gao, C. (2021). Genome-wide specificity of prime editors in plants. *Nat Biotechnol* 39, 1292–1299.
- Kusano, H., Ohnuma, M., Mutsuro-Aoki, H., Asahi, T., Ichinosawa, D., Onodera, H., Asano, K., Noda, T., Horie, T., Fukumoto, K., et al. (2018). Establishment of a modified CRISPR/Cas9 system with increased mutagenesis frequency using the translational enhancer dMac3 and multiple guide RNAs in potato. *Sci Rep* 8, 13753.
- Leffingwell, J.C. (1999). Basic chemical constituents of tobacco leaf and differences among tobacco types. Oxford: Blackwell Science.
- Li, H., Li, J., Chen, J., Yan, L., and Xia, L. (2020). Precise modifications of both exogenous and endogenous genes in rice by prime editing. *Mol Plant* 13, 671–674.
- Li, H., Zhu, Z., Li, S., Li, J., Yan, L., Zhang, C., Ma, Y., and Xia, L. (2022a). Multiplex precision genome editing by a surrogate prime editor in rice. *Mol Plant* 15, 1077–1080.
- Li, J., Chen, L., Liang, J., Xu, R., Jiang, Y., Li, Y., Ding, J., Li, M., Qin, R., and Wei, P. (2022b). Development of a highly efficient prime editor 2 system in plants. *Genome Biol* 23, 161.
- Lin, Q., Jin, S., Zong, Y., Yu, H., Zhu, Z., Liu, G., Kou, L., Wang, Y., Qiu, J.L., Li, J., et al. (2021). High-efficiency prime editing with optimized, paired pegRNAs in plants. *Nat Biotechnol* 39, 923–927.
- Lin, Q., Zong, Y., Xue, C., Wang, S., Jin, S., Zhu, Z., Wang, Y., Anzalone, A.V., Raguram, A., Doman, J.L., et al. (2020). Prime genome editing in rice and wheat. *Nat Biotechnol* 38, 582–585.
- Liu, Y., Zeng, J., Yuan, C., Guo, Y., Yu, H., Li, Y., and Huang, C. (2019). Cas9-PF, an early flowering and visual selection marker system, enhances the frequency of editing event occurrence and expedites the isolation of genome-edited and transgene-free plants. *Plant Biotechnol J* 17, 1191–1193.
- Lu, Y., Tian, Y., Shen, R., Yao, Q., Zhong, D., Zhang, X., and Zhu, J. (2021). Precise genome modification in tomato using an improved prime editing system. *Plant Biotechnol J* 19, 415–417.
- Miller, S.M., Wang, T., Randolph, P.B., Arab, M., Shen, M.W., Huang, T. P., Matuszek, Z., Newby, G.A., Rees, H.A., and Liu, D.R. (2020). Continuous evolution of SpCas9 variants compatible with non-G PAMs. *Nat Biotechnol* 38, 471–481.
- Nelson, J.W., Randolph, P.B., Shen, S.P., Everette, K.A., Chen, P.J., Anzalone, A.V., An, M., Newby, G.A., Chen, J.C., Hsu, A., et al. (2022). Engineered pegRNAs improve prime editing efficiency. *Nat Biotechnol* 40, 402–410.
- Perroud, P.F., Guyon-Debast, A., Veillet, F., Kermarrec, M.P., Chauvin, L., Chauvin, J.E., Gallois, J.L., and Nogué, F. (2022). Prime Editing in the model plant *Physcomitrium patens* and its potential in the tetraploid potato. *Plant Sci* 316, 111162.
- Qiu, F., Xing, S., Xue, C., Liu, J., Chen, K., Chai, T., and Gao, C. (2022). Transient expression of a TaGRF4-TaGIF1 complex stimulates wheat regeneration and improves genome editing. *Sci China Life Sci* 65, 731–738.
- Ren, J., Meng, X., Hu, F., Liu, Q., Cao, Y., Li, H., Yan, C., Li, J., Wang, K., Yu, H., et al. (2021). Expanding the scope of genome editing with SpG and SpRY variants in rice. *Sci China Life Sci* 64, 1784–1787.
- Sallaud, C., Giacalone, C., Töpfer, R., Goepfert, S., Bakaher, N., Rösti, S., and Tissier, A. (2012). Characterization of two genes for the biosynthesis of the labdane diterpene Z-abienol in tobacco (*Nicotiana tabacum*) glandular trichomes. *Plant J* 72, 1–17.
- Seo, S., Gomi, K., Kaku, H., Abe, H., Seto, H., Nakatsu, S., Neya, M., Kobayashi, M., Nakaho, K., Ichinose, Y., et al. (2012). Identification of natural diterpenes that inhibit bacterial wilt disease in tobacco, tomato and *Arabidopsis*. *Plant Cell Physiol* 53, 1432–1444.

- Severson, R., Johnson, A., and Jackson, D. (1985). Cuticular constituents of tobacco: factors affecting their production and their role in insect and disease resistance and smoke quality. *Recent Adv Tobacco Sci* 11, 105–174.
- Severson, R.F., Arrendale, R.F., Chortyk, O.T., Johnson, A.W., Jackson, D. M., Gwynn, G.R., Chaplin, J.F., and Stephenson, M.G. (1984). Quantitation of the major cuticular components from green leaf of different tobacco types. *J Agric Food Chem* 32, 566–570.
- Sretenovic, S., Yin, D., Levav, A., Selengut, J.D., Mount, S.M., and Qi, Y. (2021). Expanding plant genome-editing scope by an engineered iSpyMacCas9 system that targets A-rich PAM sequences. *Plant Commun* 2, 100101.
- Tan, J., Zeng, D., Zhao, Y., Wang, Y., Liu, T., Li, S., Xue, Y., Luo, Y., Xie, X., Chen, L., et al. (2022). PhieABEs: a PAM-less/free high-efficiency adenine base editor toolbox with wide target scope in plants. *Plant Biotechnol J* 20, 934–943.
- Tang, X., Sretenovic, S., Ren, Q., Jia, X., Li, M., Fan, T., Yin, D., Xiang, S., Guo, Y., Liu, L., et al. (2020). Plant prime editors enable precise gene editing in rice cells. *Mol Plant* 13, 667–670.
- Walton, R.T., Christie, K.A., Whittaker, M.N., and Kleinstiver, B.P. (2020). Unconstrained genome targeting with near-PAMless engineered CRISPR-Cas9 variants. *Science* 368, 290–296.
- Wang, G.P. (2016). Functional analysis and marker development of *cis*-abienol synthesis gene in tobacco (in Chinese). Dissertation for Master's Degree. Beijing: Chinese Academy of Agricultural Sciences.
- Wang, L., Kaya, H.B., Zhang, N., Rai, R., Willmann, M.R., Carpenter, S.C. D., Read, A.C., Martin, F., Fei, Z., Leach, J.E., et al. (2021). Spelling changes and fluorescent tagging with prime editing vectors for plants. *Front Genome Ed* 3, 617553.
- Wang, M., Xu, Z., Gosavi, G., Ren, B., Cao, Y., Kuang, Y., Zhou, C., Spetz, C., Yan, F., Zhou, X., et al. (2020a). Targeted base editing in rice with CRISPR/ScCas9 system. *Plant Biotechnol J* 18, 1645–1647.
- Wang, W.G., Wang, H., Du, L.Q., Li, M., Chen, L., Yu, J., Cheng, G.G., Zhan, M.T., Hu, Q.F., Zhang, L., et al. (2020b). Molecular basis for the biosynthesis of an unusual chain-fused polyketide, gregatin A. *J Am Chem Soc* 142, 8464–8472.
- Xu, J., Yin, Y., Jian, L., Han, B., Chen, Z., Yan, J., and Liu, X. (2021). Seeing is believing: a visualization toolbox to enhance selection efficiency in maize genome editing. *Plant Biotechnol J* 19, 872–874.
- Xu, R., Li, J., Liu, X., Shan, T., Qin, R., and Wei, P. (2020a). Development of plant prime-editing systems for precise genome editing. *Plant Commun* 1, 100043.
- Xu, R., Qin, R., Xie, H., Li, J., Liu, X., Zhu, M., Sun, Y., Yu, Y., Lu, P., and Wei, P. (2022a). Genome editing with type II-C CRISPR-Cas9 systems from *Neisseria meningitidis* in rice. *Plant Biotechnol J* 20, 350–359.
- Xu, W., Zhang, C., Yang, Y., Zhao, S., Kang, G., He, X., Song, J., and Yang, J. (2020b). Versatile nucleotides substitution in plant using an improved prime editing system. *Mol Plant* 13, 675–678.
- Xu, W., Yang, Y., Yang, B., Krueger, C.J., Xiao, Q., Zhao, S., Zhang, L., Kang, G., Wang, F., Yi, H., et al. (2022b). A design optimized prime editor with expanded scope and capability in plants. *Nat Plants* 8, 45–52.
- Yan, Y., Zhu, J., Qi, X., Cheng, B., Liu, C., and Xie, C. (2021). Establishment of an efficient seed fluorescence reporter-assisted CRISPR/Cas9 gene editing in maize. *J Integr Plant Biol* 63, 1671–1680.
- Yuan, G., Hassan, M.M., Yao, T., Lu, H., Vergara, M.M., Labbé, J.L., Muchero, W., Pan, C., Chen, J.G., Tuskan, G.A., et al. (2021). Plant-based biosensors for detecting CRISPR-mediated genome engineering. *ACS Synth Biol* 10, 3600–3603.
- Zerbe, P., and Bohlmann, J. (2015). Enzymes for synthetic biology of ambroxide-related diterpenoid fragrance compounds. *Adv Biochem Eng Biotechnol* 148, 427–447.
- Zhang, C., Wang, F., Zhao, S., Kang, G., Song, J., Li, L., and Yang, J. (2020). Highly efficient CRISPR-SaKKH tools for plant multiplex cytosine base editing. *Crop J* 8, 418–423.
- Zhang, C., Wang, Y., Wang, F., Zhao, S., Song, J., Feng, F., Zhao, J., and Yang, J. (2021). Expanding base editing scope to near-PAMless with engineered CRISPR/Cas9 variants in plants. *Mol Plant* 14, 191–194.
- Zong, Y., Liu, Y., Xue, C., Li, B., Li, X., Wang, Y., Li, J., Liu, G., Huang, X., Cao, X., et al. (2022). An engineered prime editor with enhanced editing efficiency in plants. *Nat Biotechnol* 40, 1394–1402.
- Zou, J., Meng, X., Liu, Q., Shang, M., Wang, K., Li, J., Yu, H., and Wang, C. (2022). Improving the efficiency of prime editing with epegRNAs and high-temperature treatment in rice. *Sci China Life Sci* 65, 2328–2331.

SUPPORTING INFORMATION

The supporting information is available online at <https://doi.org/10.1007/s11427-022-2396-x>. The supporting materials are published as submitted, without typesetting or editing. The responsibility for scientific accuracy and content remains entirely with the authors.